Contents lists available at ScienceDirect

Virology

An extension of the Minute Virus of Mice tissue tropism

Igor Etingov [a,*], Refael Itah [a,1], Michal Mincberg [a,1], Ayelet Keren-Naus [a,1], Hyun-Joo Nam [b,2], Mavis Agbandje-McKenna [b,2], Claytus Davis [a,1]

[a] Department of Virology and Developmental Molecular Genetics, Faculty of Health Sciences, Ben-Gurion University of the Negev, Beer Sheva, Israel
[b] Department of Biochemistry and Molecular Biology, College of Medicine, University of Florida, Gainesville, FL 32610-0245, USA

A B S T R A C T

Well-defined tissue tropism makes Autonomous Parvoviruses a valuable model for studies of virus–cell interactions and gene therapy research. We developed a new Minute Virus of Mice variant, different from the known prototype (MVMp) and immunosuppressive (MVMi) strains. The new virus variant, designated F1, was isolated from the culture of semi-permissive Fisher Rat Fibroblasts, F111, infected with MVMp. The F1 genome carried point mutations in regions known to determine the mutually restricted host ranges of MVMp and MVMi. In F111 cells, F1 cytotoxicity, gene expression and multiplication were significantly higher compared to MVMp. Conversely the wild-type virus propagated in MVMp-permissive cells more efficiently than the F1. Reversion of the F1-specific mutations to wild-type MVMp sequence, following reverse-passaging of the mutant virus in MVMp-permissive cells, confirmed a specific adaptation of the F1 virus to F111 cells. Considerable divergence in tissue specificities between the wild-type and mutant viruses was demonstrated in vivo.

© 2008 Elsevier Inc. All rights reserved.

Introduction

Minute Virus of Mice (MVM) belongs to the Autonomous Parvoviruses (APVs), some of the smallest known animal viruses. Their main common features are a single-stranded DNA genome of about 5.1 kb with small terminal palindromes and icosahedral capsids approximately 26 nm in diameter (Tattersall, 2006). Two APV properties have drawn a lot of interest during the last three decades. The dependence of APVs on both cellular proliferation factors, expressed throughout S-phase, and the differentiation of host cells to achieve lytic infection make them predominantly propagate in rapidly dividing cells, sometimes achieving a remarkable oncotropism (Cornelis et al., 2006). Although APV hosts are widely spread in the animal kingdom, some parvovirus species are known to consist of several strains, possessing different pathological spectra (Parrish and Hueffer, 2006). Thus parvoviruses serve as a valuable model for the study of virus–host interactions. In addition, the possibility of constructing viruses with recombinant genomes (vectors), carrying non-viral genes, makes APVs prominent objects for gene therapy research (Cornelis and Dinsart, 2006).

The MVM genome is replicated via double-stranded intermediates and a rolling-hairpin mechanism (Cotmore and Tattersall, 2006). This includes conversion of the single-stranded genome (ss, ~5.1 kb) into a double-stranded (ds) monomer replicative form (mRF, ~5 kb), subsequent synthesis of a dimer form — dRF (dsDNA ~10 kb), containing two copies of the original genome, as well as additional intermediates. Finally, this is followed by resolution and packaging of ss genomes. Both viral nonstructural proteins (NS) and cellular factors, expressed in the S-phase, are necessary for the process.

The MVM genes are organized into two overlapping transcription units with promoters located at map units (m.u.) 4 (P4) and 38 (P38) (Pintel et al., 1983) transcribing three main mRNAs. P4 controls synthesis of R1 (4.8 kb) and R2 (3.3 kb), while P38 regulates R3 (3 kb) production. R1 and R2 are produced from the same pre-mRNA, but R2 lacks the large intron between m.u. 10 and 39. All three mRNAs undergo splicing of the small intron between m.u. 46 and 48 (Qiu et al., 2006). NS1 (83 kDa) and NS2 (24 kDa) are translated from R1 and R2 respectively (Cotmore and Tattersall, 1986). Both of these are necessary for virus replication and cytotoxicity (Nuesch, 2006). All capsid proteins are synthesized from R3 transcripts. VP1 (83 kDa) and VP2 (64 kDa) are produced by alternative splicing, while VP3 (comprising about 90% of virus full capsids) is generated by posttranslational cleavage following DNA packaging (Tattersall et al., 1977).

The P4 and P38 promoters possess similar basic promoter elements: SP1 binding sites, TATA boxes, and putative initiator sequences (Lorson and Pintel, 1997). P4 contains several additional regulatory sequences, and may be expressed in the absence of viral proteins

* Corresponding author. Fax: +972 8 627 6215.
  E-mail addresses: etingov@bgu.ac.il (I. Etingov), refaelit@zahav.net.il (R. Itah), mincberg@bgu.ac.il (M. Mincberg), aynaus@bgu.ac.il (A. Keren-Naus), mckenna@ufl.edu (M. Agbandje-McKenna), clay@bgu.ac.il (C. Davis).
  [1] Fax: +972 8 627 6215.
  [2] Fax: +1 352 392 3422.

(Faisst et al., 1994). In contrast, P38 exhibits exceptionally low basal expression, but can be upregulated (~100 fold) by NS1, which acts as a transcriptional activator (Doerig et al., 1988), binding to a specific DNA regulatory sequence at the promoter (Cotmore et al., 1995).

MVM serves as a good model of parvoviral strain-specific variation. The prototype (MVMp) and immunosuppressive (MVMi) strains efficiently propagate in cultured mouse fibroblasts and T lymphocytes, respectively. Their host ranges are reciprocally restricted, although they are serologically indistinguishable and exhibit only ~3% DNA sequence divergence (Tattersall and Bratton, 1983). Significant differences in the tissue tropisms of these two MVM strains were also found in newborn mice (Kimsey et al., 1986) and mouse embryos (Itah et al., 2004b).

The mechanism restricting infection of MVMp and MVMi in each other's host cells is not fully understood, but is considered to be intracellular, rather than occurring on the outer cell membrane (Spalholz and Tattersall, 1983; Previsani et al., 1997). There are at least two kinds of host range determinants, one located in capsid coding region and the other in the large-intron 3′ splice site, that are responsible for MVM fibrotropism. Recombinant MVMi carrying two amino acids specific to MVMp in the capsid coding region (at the VP2 positions 317 and 321) was shown to infect fibroblasts more than 100 times better than the original MVMi (Gardiner and Tattersall, 1988). Either of these substitutions, complemented with additional changes (defined as second-site mutations), was shown to confer fibrotropism on MVMi. Structurally, the 317 and 321 VP2 amino acids, as well the second-site mutations are associated with a dimple-like depression located at the icosahedral two-fold axis in the MVM capsid. This site was proposed to be involved in the interaction of the viral particles with sialic acid, crucial for infection (Agbandje-McKenna et al., 1998; López-Bueno et al., 2006a). The second host determinant establishes the ability of the virus genome to express NS2. A silent guanine to adenine substitution in MVMi at nt 1970 was demonstrated to cause a dramatic increase in NS2 levels via increased large-intron splicing in mouse fibroblasts. This correlated with elevated virus ssDNA (Choi et al., 2005). The same mutation and a similar substitution at nt 1967 were found in MVMi mutants with plaque forming capability in fibroblast monolayers (D'Abramo et al., 2005).

It is not known what the adaptive cell-type range of MVM or other autonomous parvoviruses is. It has been shown that forced culture (persistent infection) of MVMi in mouse fibroblasts can lead to an acquired fibrotropism (Ron et al., 1984). The objective of this work was to further characterize the adaptive range of MVM through persistent infection of non-murine cells that are restrictive to the wild-type virus. Prolonged MVMp infection of F111 Fisher Rat Fibroblasts resulted in the preferential selection of a mutant virus, called F1. This mutant was shown to be specifically adapted to propagation in F111 cells in vitro, and its in vivo host range diverged considerably from that of wild-type MVMp. We describe here the derivation of F1, its infection in F111 and normal MVM hosts compared to the parental MVMp. Sequencing and expression studies showed the effect of the observed genome alterations on the infection parameters in tissue culture and in vivo. Structural mapping localized the coat protein residues mutated in the F1 virus to the sialic acid binding region at the icosahedral two-fold axis of the MVM capsid.

Results

Adaptation of MVMp to rat fisher embryonic fibroblasts (F111 cells)

We tested the ability of MVMp to extend its tropism to a non-murine, semi-permissive host cell-type, F111 rat fibroblasts. These cells were infected with 2 PFU/cell of transfection-derived MVMp (Materials and methods). A moderate cytopathic effect (CPE) appeared 3 days post infection (dpi), followed by quick culture recovery (4–5 dpi) and subsequent normal cell growth. However, despite normal cell growth, cell cultures at 14 dpi contained virus — as determined by plaque assays in A9 cells. Infection of naive F111 cells with 14 dpi virus led, once again, to mild cell death followed by full recovery of the culture. DNA sequencing of F111-extracted viral samples revealed no differences from the wild-type (WT) MVMp genome.

We hypothesized that increased divergence of the initial viral population could increase chances of successful selection of adaptive changes. We reasoned that multiple cycles of infection in a permissive host should create the high genetic heterogeneity that has been reported for the parvoviruses (López-Bueno et al., 2006b). We therefore cultured transfection-derived MVMp virus through 5 successive passages in permissive A9 cells (Materials and methods). F111 cells infected with this A9-passaged virus (MVMp-A9) exhibited no differences in CPE compared to infection with the transfection-derived MVMp. However, virus extracted following 14 days of prolonged MVMp-A9 infection in F111 cells (designated as MVMp-F111) was capable of effectively destroying naive F111 cell cultures, unlike transfection-derived MVMp or MVMp-A9 (Supplementary material, Fig. 8).

Purification and sequencing of F111-adapted virus

Sequencing of MVMp-F111 led to ambiguous results, presumably because of genomic heterogeneity. Therefore virus was purified both by end-point dilution in F111 cells and plaque purification in A9 cells. 14 of 20 plaque-purified samples and all end-point dilution isolates destroyed F111 cultures upon infection. The plaque purification results likely reflected genomic heterogeneity of the MVMp-F111 population, whereas only subpopulation/s with the ability to destroy F111 culture could be isolated by end-point dilution in these cells.

Viral DNA from 5 plaque-purified samples, with the ability to kill F111 cells, and 5 end-point dilution isolates were sequenced and a single mutational pattern, designated F1, was revealed (Table 1). 4 of 5 identified mutations occurred on the capsid protein coding sequence, leading to amino acid changes. One mutation, G1955A, was located within the NS1 coding sequence, near the large splice branch-point, and within the consensus SP1 binding site of the P38 promoter. With respect to translation, the substitution is silent (Fig. 1A).

Locations of F1 mutations on the 3D structure of MVMp capsid (VP2)

As shown in Fig. 1B, the four mutations in F1 that resulted in amino acid changes in VP regions of the coat protein (Table 1) were mapped onto the MVMp structure determined by X-ray crystallography (Kontou et al., 2005), in order to evaluate the structural impact of the changes at a tertiary and quaternary protein structure level. Residue A334, buried inside the capsid, has a side-chain that points into a hydrophobic pocket and is involved in the stabilization of three-fold inter-subunit interactions. The three remaining amino acid residues, E384, N554 and I578, are located on the capsid surface, clustering around the depressions at the icosahedral two-fold axis of

Table 1
Mutations found in the F1 mutant virus

Nucleotide position (bp)	Nucleotide change	VP change (amino acid)	VP1 amino acid position	VP2 amino acid position
1955	G to A	–	–	–
3793	G to A	Ala to Thr	476	334
3944	A to C	Glu to Ala	526	384
4453	A to G	Asn to Asp	696	554
4525	A to C	Ile to Leu	720	578

PCR amplification products of the packaged virus DNA were sequenced (Materials and methods). Positions of nucleotide changes are indicated according to the GenBank MVMp sequence (accession number J02275). Amino acid changes are indicated relative to GenBank MVMp sequences (NP_041244.1 and NP_041248.1 for VP1 and VP2, respectively).
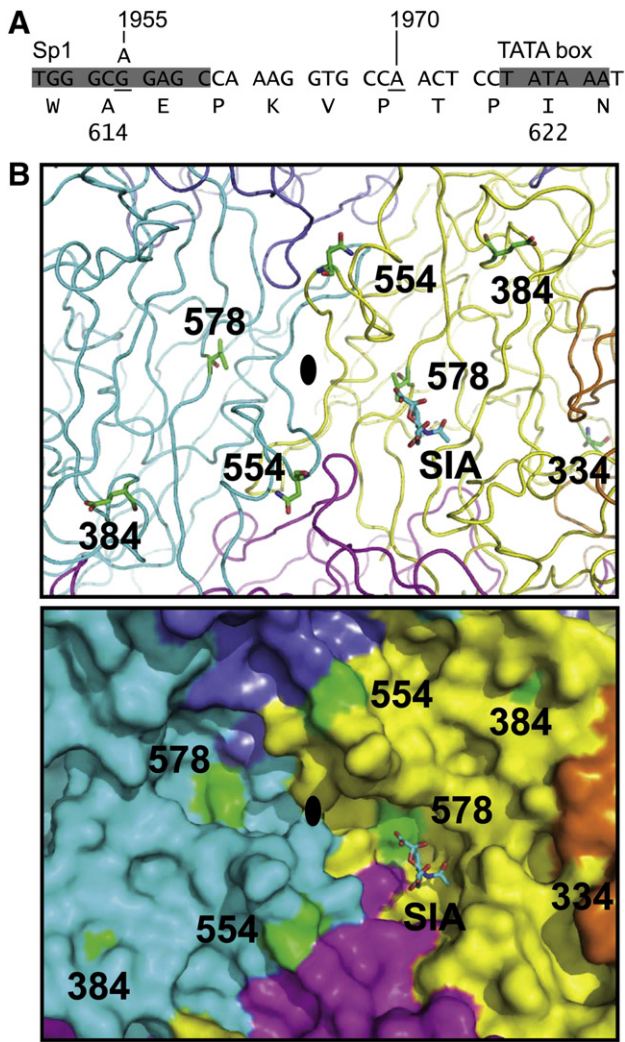
Fig. 1. Representation of alternations found in the F1 mutant. (A) P38 promoter region. The DNA sequence and its corresponding NS1 amino acid sequence are represented according to GenBank sequences J02275 and NP_041242, respectively. Locations of the G1955A substitution, found in F1, of A1970, the branch point for excision of the large intron from NS-coding pre-mRNA in A9 cells (Choi et al., 2005), and of core promoter elements are indicated. (B) Mutated VP residues, found in F1 (Table 1) were mapped onto the X-ray crystal structure model of the MVMp capsid (residues 39–587). The top panel shows a stick representation of the 4 residues (in green) in the context of the backbone trace of the VP2 polypeptides shown in the different colors for icosahedral symmetry related monomers (yellow), cyan (two-fold), orange and magenta (three-fold), and bluish purple (five-fold). The bottom panel shows the same view with a surface representation. The sialic acid mapped onto the MVMp capsid surface (López-Bueno et al., 2006a,b) is shown in both panels in the right-hand-side two-fold pocket, with the carbons in cyan, the oxygens in red and the nitrogens in blue. The two-fold axis is shown with the filled oval.

the capsid, in the vicinity of a structurally mapped putative sialic acid receptor binding site in MVMp (Fig. 1B). E384 is located in a surface loop at the shoulder of the protrusions at the icosahedral three-fold axes and is involved in interactions with S388 and P392 that are likely required for stabilizing the conformation of their loop. Residue S388 is an MVMp/MVMi differing residue that has not yet been implicated in their tissue tropism differences. N554 and I578 are located on the wall and floor, respectively, of the two-fold dimple depression on the capsid surface, also within the vicinity of the sialic acid receptor binding site (Fig. 1B) (López-Bueno et al., 2006a).

CAT reporter gene assay of the mutant P38 promoter

We hypothesized that the silent substitution, G1955A, (Fig. 1A) would affect viral gene expression, as it lies within the consensus SP1

binding site of the P38 promoter. To test this we transfected mutant and WT CAT reporters into different host cells. Two promoter/reporter constructs containing the CAT sequence under control of a WT (pP38-[WT]) or mutant (pP38-[1955]) P38 promoter were made. An additional plasmid, pNS, expressing the viral NS1 protein, which activates P38 expression (Doerig et al., 1988), was also constructed (Materials and methods). pNS and the P38-reporter plasmids were co-transfected into different host cells and CAT activity measured after 48 h (Fig. 2). The results showed that the 1955 substitution caused a marginal, but sometimes significant, reduction in P38 activity in all checked cell-types, including F111 cells (Fig. 2). The data suggest that this mutation likely contributes to F1 adaptation by some other way than altering its P38 expression in F111 rat fibroblasts, such as an elevated accumulation of NS2.

Virus quasispecies during culture and host cell-type shifts

To identify and follow the relative frequencies of the characterized sequence variants during propagation in different cell cultures, we adapted an ARMS allele-specific PCR technique (Newton et al., 1989). For each variant location, selective and unselective ARMS primers were designed (Table 3) and used for allele-specific PCR. It was possible to specifically amplify WT or mutant plasmid DNA templates in quantities ranging from 0.1 fg ($\sim$20 plasmid molecules) to 10 ng ($\sim 2*10^9$ molecules) and effectively identify alleles in mixed WT and mutant DNA pools in ratios of $1:10^8$, for each of the variant loci (Fig. 3A). Although the assay is not strictly quantitative we consistently obtained easily identifiable distinctions among quantities of PCR products when significantly different template amounts were used for reactions, indicating that the ARMS could reliably assay divergence in quasispecies content for each variation identified in our viral samples.

The calibrated allele-specific ARMS PCR was used to characterize the sequence variants present in populations of viruses isolated from our culture experiments. The initial selection experiments indicated that F1 mutant virus arose only from MVMp that had been passaged in A9 cells (MVMp-A9), not from virus produced directly following transfection of the infectious cloned MVMp (MVMp-pMM984) (Materials and methods). We hypothesized that MVMp adaptation to the F111 cells occurred through selection of quasispecies present in the MVMp-A9 population. We therefore characterized the frequency of the sequence variants in the different viral stocks by ARMS. The data show that the variants selected during F111 cell culture were present in MVMp-A9, but not in MVMp-pMM984 (Fig. 3B). Although MVMp-F111 virus consisted of mixed WT and mutant subpopulations, only mutant loci were detected in its end-point dilution isolate (F1-EPD). Subsequent propagation of this isolate in F111 cells to obtain sufficient
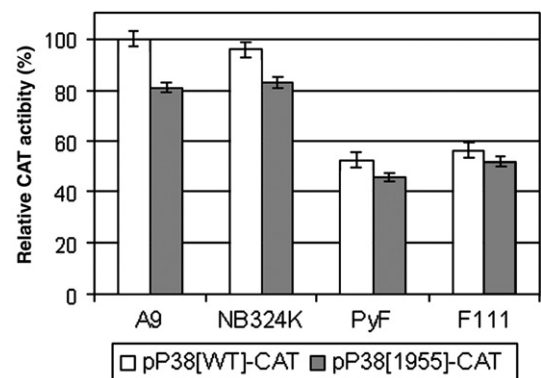

Fig. 2. Wild-type G1955 and mutant 1955A promoter activity. 10^5 F111, A9, NB324K, or PyF cells were co-transfected with the indicated CAT construct, pNS and pSV2βgal (as an internal control of transfection). Relative CAT activities are represented as percentages of the normalized CAT activity achieved by pP38[WT]-CAT in A9 cells. Error bars show the standard deviation for 3 independent replicates.

A

1955 bp G to A substitution

4453 bp G to A substitution

B

1955 bp G to A substitution

4453 bp G to A substitution

C

1955 bp G to A substitution

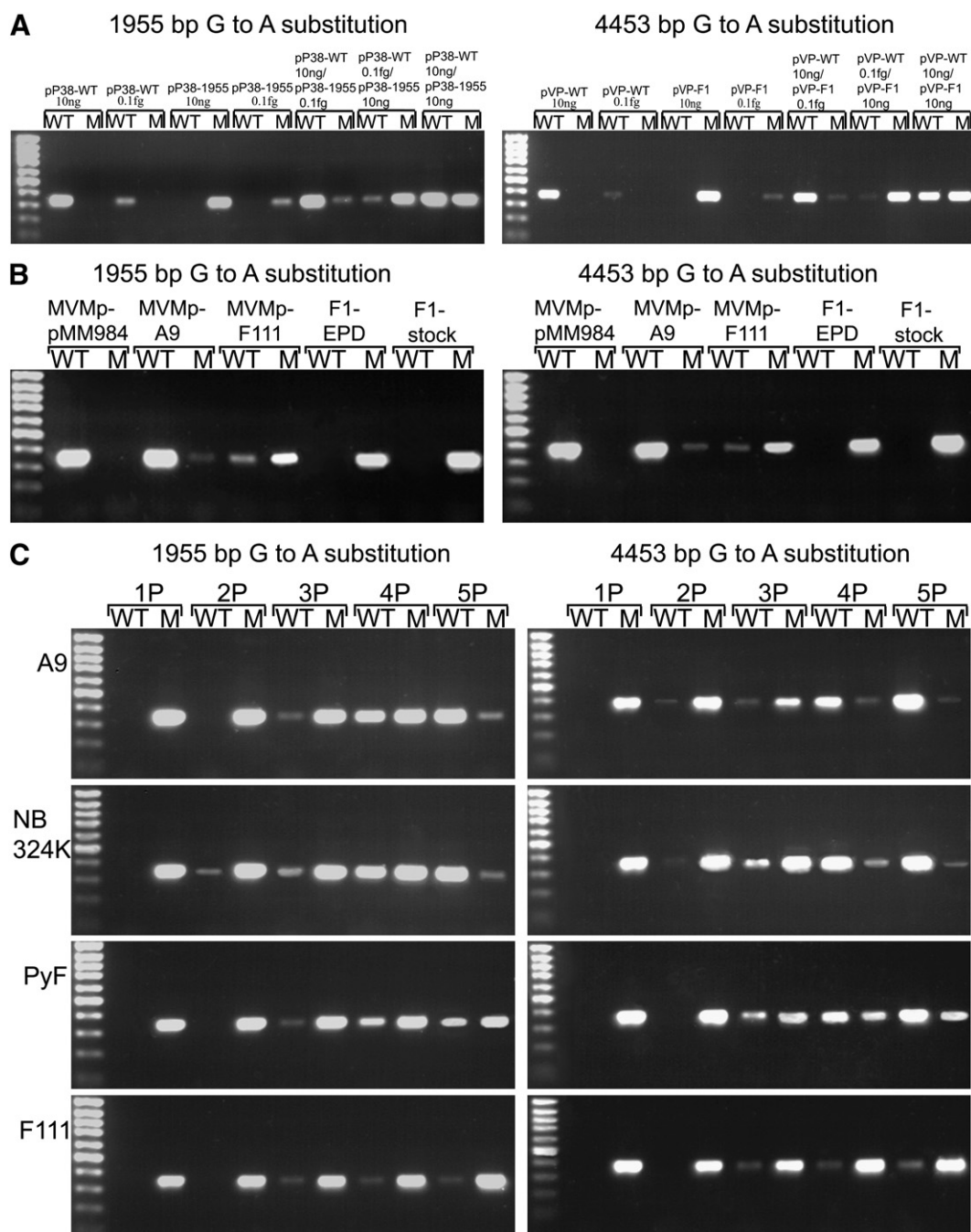4453 bp G to A substitution

Fig. 3. ARMS calibration and analysis of virus samples. In each allele-specific PCR (35 cycles), a selective primer for either wild-type (WT) or mutant (M) template, along with the conventional unselective primer (Table 3), was used. Results of tests for 1955 and 4453 bp positions are shown. Reaction products and 100 bp DNA Ladder (New England BioLabs) were resolved by 1.5% agarose gel electrophoresis. (A) ARMS specificity test. Plasmids with cloned wild-type MVMp DNA (pP38-WT, pVP-WT), plasmids carrying F1 mutant pattern (pP38-1955, pVP-F1), or plasmid mixtures in the indicated quantities were tested with ARMS. (B) Presence of the wild-type and mutant DNA in viral samples. The indicated viral samples (see text) were checked with ARMS. (C) Sequence selection during serial passage of mutant virus in different host cell-types. F1 mutant virus was serially passaged 5 times (1P–5P) in the indicated cell lines. At each passage, $4*10^5$ cells were infected with 0.2 PFU/cell. After cell culture death, virus was extracted and ARMS performed.

quantity of the mutant virus (F1-stock) did not cause any detectable reversion of the F1 mutations to WT (Fig. 3B).

If the F1 mutations that became predominant following culture in F111 rat fibroblasts were an adaptive response to a poorly permissive host, we reasoned that these changes would be preserved during F1 propagation in these cells, but that repeated infections of known MVMp hosts cells with F1 would result in reversion — the appearance and enrichment of a WT MVMp subpopulation. To check this hypothesis we passaged F1 in A9, NB324K, PyF and F111 cells 5 times. 2–3 passages (4–6 cycles of infection) of virus in all of these host cell-types

led to the appearance of quasispecies, with reversion toward the WT MVMp pattern (Fig. 3C). These subpopulations were continuously enriched during subsequent passages in A9 and NB324K cells, and clearly dominated the viral populations after the 5th passage (~10 infection cycles). Passaging of F1 in PyF cells also resulted in the appearance of WT sequence. However, after 5 passages, (Fig. 3C) subpopulation/s carrying F1 mutations still composed a significant fraction of the viral sample and after further 5 passages F1-specific sequence was still clearly present (data not shown). Although quasispecies with WT sequence appeared also during the F1
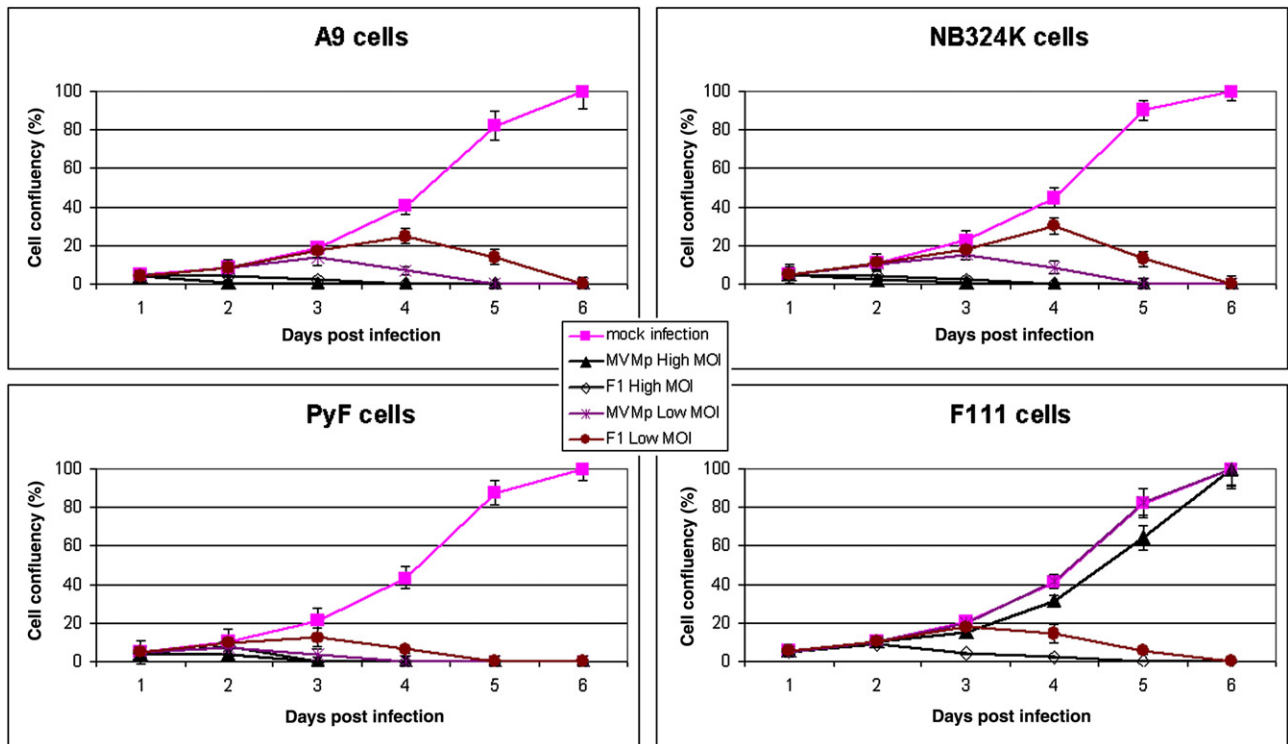
Fig. 4. Cell culture confluency following MVMp and F1 infection. 2000 A9 or NB324K cells in 96 well microtiter plates were infected with 2 PFU/cell (High MOI) or 0.2 PFU/cell (Low MOI) of MVMp or F1. Confluency of surviving cells was measured spectrophotometrically by MTT assay (Materials and methods). Bars represent the standard deviations in 10 independent trials.

propagation in F111 cells, their level was low and F1 remained dominant (Fig. 3C). Although allele compositions are illustrated for the variant loci at nt 1955 and 4453, similar results were obtained for the other alleles at nt 3793, 3944 and 4525 (data not shown).

Infection characteristics of F1 in comparison with wild-type MVMp

To examine the effects of the suite of selected mutations on infectivity, we characterized the responses of different host cells to infection by parental and variant viruses. A cell survival test (Fig. 4) showed that F1-killing of A9, NB324K and PyF cells was undistinguishable from WT MVMp at high MOI (2 PFU/cell). However, infections with low MOI (0.2 PFU/cell) demonstrated a significant delay in the destruction of these cultures by F1 compared with WT MVMp (Fig. 4). F1 also exhibited significantly lower infectious viral particle production in MVMp-permissive cells compared to WT virus (Table 2). A diminished ability of F1 to propagate in A9 and NB324K cells was verified by comparing the plaque morphology of the WT and mutant viruses on monolayers of these cells. Plaques formed by F1 were significantly smaller than those formed by MVMp (Supplementary material, Fig. 9). Infections of F111 cells confirmed that only F1 was capable of destroying these cells (Fig. 4), and that F1 propagates in

Table 2
Active viral particle production by different cell lines (PFU/cell)

Virus	Cells			
	A9	NB324K	PyF	F111
MVMp	1120 (±43)	1051	670 (±19)	0.4 (±0.02)
F1	88 (±4.2)	69 (±2)	310 (±9.1)	21 (±0.7)

10^6 cells of each type were infected by WT MVMp or the F1 mutant with a MOI 2 PFU/cell. 3 dpi virus was extracted and plaque assays were performed in A9 cells (Materials and methods). Numbers in brackets are standard deviations calculated from 5 independent infections.
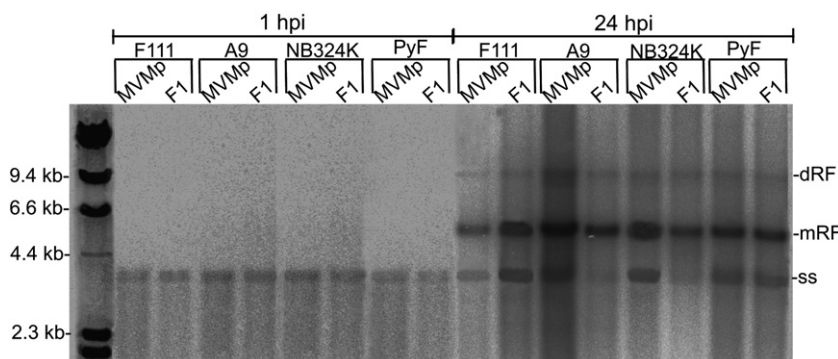
these rat fibroblasts significantly more efficiently than WT MVMp (Table 2).

Host-dependent differences in viral products during MVMp and F1 infection

To better understand the effects of the naturally selected variations on the viral lifecycle we compared some of the major parameters of MVM infection by F1 and the WT virus. Both virus strains were used to infect rat F111 and PyF cells, as well as the typical WT MVMp hosts, A9 and NB324K cells. Low molecular weight DNA was extracted at 1 and 24 h following infection and MVM genomic DNA detected by Southern blot (Fig. 5). As might be expected from selection and cytotoxicity results in F111 rat fibroblasts, the level of F1 DNA replication forms (RF) in these cells was significantly higher than that of wild-type MVMp. Vice versa, the infection of MVMp-permissive cells A9 and NB324K showed preferential WT virus replication (Fig. 5, 24 hpi assays). Cell extracts prepared 1 h after infection contained similar quantities of the virus genomic single-stranded (ss) DNA (Fig. 5, 1 hpi assays). The source of ssDNA at this early stage of infection, in the absence of any detectable RF could be only MVM packaged genomic DNA, i.e. the inoculum, indicating that there is no significant difference between the binding abilities of WT and mutant viruses to the surfaces of any of the checked cell-types. The similar levels of ssDNA 1 h after infection and the considerable differences in replication levels 24 hpi suggest that the infections of WT MVMp in F111 and the F1 variant in A9 and NB324K cells are reciprocally impaired at some stage between capsid attachment to a cell and virus DNA replication. Finally it was likely that this difference is transformation-dependent; WT MVMp replication was moderately higher in PyF cells than the replication of F1.

We characterized the products of MVMp and F1 gene expression by Northern and Western analyses at 14 and 24 h post-infection respectively (Fig. 6). Higher levels of F1 genome expression products

Fig. 5. Wild-type MVMp and F1 mutant DNA replication. F111, A9, NB324K, or PyF cell cultures were infected with 2 PFU/cell of either wild-type MVMp or mutant F1 virus. Low molecular weight DNA was extracted one and 24 h after infection (hpi). Extracted DNA from 10^4 cells and a Lambda-HindIII DNA size marker (NEB) were resolved by 0.8% agarose gel electrophoresis and subjected to Southern blot analysis using mixed MVMp and Lambda labeled DNA as a probe. dRF — dimer replicative form, mRF — monomer replicative form, ss — single-stranded genome.

(from both P4 and P38 promoters) were observed in F111 cells, while significantly increased amounts of MVMp mRNA and proteins were expressed in A9 and NB324K cells. MVMp was found to have only slightly increased expression from either of its promoters compared to F1 in PyF cells (Fig. 6). WT MVMp expression of R2 mRNA and NS2 protein (synthesized from R2) appeared to be particularly weakened in F111 rat fibroblasts, even as F1 infection produced significantly higher quantities of R2 and NS2 in these cells (Figs. 6A and B, respectively).

Differences between the in vivo host ranges of MVMp and F1

Because of the limited infection of Minute Virus of Mice in normal adult mice, we used an *in utero* injection technique (Itah et al., 2004a) to characterize differences in the host cell-type range in vivo. Viral inoculation of mouse embryos at 12 dpc revealed infection of bone

Fig. 6. Wild-type MVMp and F1 mutant genome expression. (A) Transcription assay. F111, A9, NB324K, or PyF cell cultures were infected with 2 PFU/cell of either wild-type MVMp or mutant F1 virus. mRNA was extracted 14 h later. 100 ng of mRNA was resolved by formaldehyde agarose (1%) gel electrophoresis. A Northern analysis was performed using wt MVMp labeled genomic DNA as a probe. R1 — NS1-encoding P4 transcript, R2 — spliced, NS2-encoding P4 transcript, R3 — structural protein P38 transcript. (B) NS protein expression. The indicated cell cultures were infected with 2 PFU/cell of either wild-type MVMp or mutant F1 virus. 24 hpi total protein was extracted and spectrophotometrically quantified. Samples of 10 µg of total protein were resolved by discontinuous SDS-Polyacrylamide gel (10%) electrophoresis. NS1 and NS2 proteins were detected by Western analysis using anti-NS polyclonal antisera and a peroxidase-labeled anti-rabbit secondary Ab. (C) Capsid protein expression. Total protein was produced as for NS. Samples of 10 µg of total protein were resolved by discontinuous SDS-Polyacrylamide gel (8%) electrophoresis. VP1 and VP2 proteins were detected by Western analysis using anti-VP polyclonal antisera and peroxidase-labeled anti-rabbit secondary Ab.

primordia by F1, that unlike the parental MVMp was accompanied by significant tissue destruction (Fig. 7A). In contrast, F1 exhibited reduced infection of skin fibroblasts (Fig. 7B) and no apparent infection in either CNS or PNS (data not shown), tissues that both exhibited sporadic infection with MVMp (Itah et al., 2004b).

A preliminary study of MVMp and F1 infection, using the neonate oronasal inoculation model (Kimsey et al., 1986) also indicated some divergence between MVMp and F1 infection patterns (Supplementary material, Fig. 10).

Discussion

Extension of MVM tropism as a result of quasispecies enrichment

Minute Virus of Mice has been shown to readily adapt to new host environments both in cell culture (Ron et al., 1984) and in vivo (López-Bueno et al., 2003). Darwinian selection apparently leads to a shift in predominant virus variants in MVM populations as a result of environmental constraints such as a new host or treatment with antibodies against MVM capsid. We show here that the same principle could be exploited to adapt MVM to non-murine, poorly permissive cells. F111, a rat fibroblast cell-line, is restrictive (semi-permissive) for MVMp (Guetta et al., 1990). The prolonged infection of F111 with MVMp led to the predominance of an adapted variant, designated as F1. In contrast to the parental MVMp, F1 destroyed F111 fibroblast cultures.

The analysis was informative with respect to the mechanics and speed of the adaptive process. F1 arose in F111 cells infected with MVMp only if the inoculating MVMp was derived from successive infection cycles in a permissive host. F1 did not arise in F111 cells infected with standard transfection-derived MVMp (Materials and methods). We suggested that the successful enrichment and eventual domination of the F1 mutant was due to the presence of quasispecies in the initial virus sample used for the infection of F111 cells. This was confirmed by allele-specific PCR (ARMS), that demonstrated the presence of all F1-specific nucleotide substitutions in A9 passaged MVMp, but not in transfection-derived virus samples.

Finally, F1 adaptation to the F111 cells was a coevolutionary process. Persistently infected rat fibroblasts sustained a normal rate of cell growth, without any signs of CPE, for the entire period of the persistent infection (we maintained the infected culture growth up to 2 months), with continuous production of the mutant virus, revealing the resistance of the culture to this mutant. In contrast, virus extracted from such cultures destroyed naive F111 cells.

The F1 mutant genome

The locations of the F1 mutations in the MVM genome indicate that adaptive determinants for F1 in rat fibroblast F111 cells are in
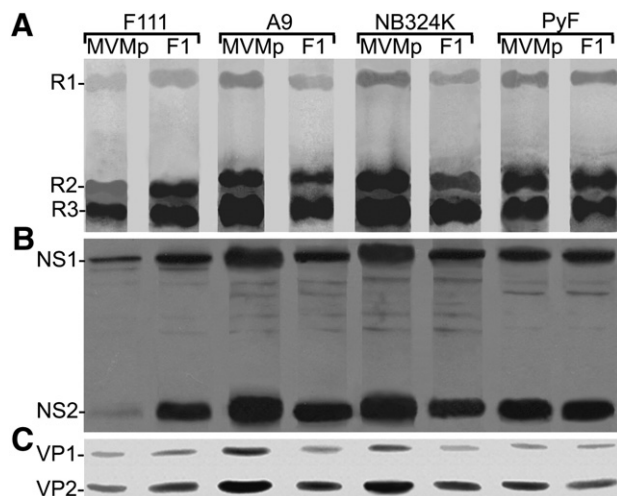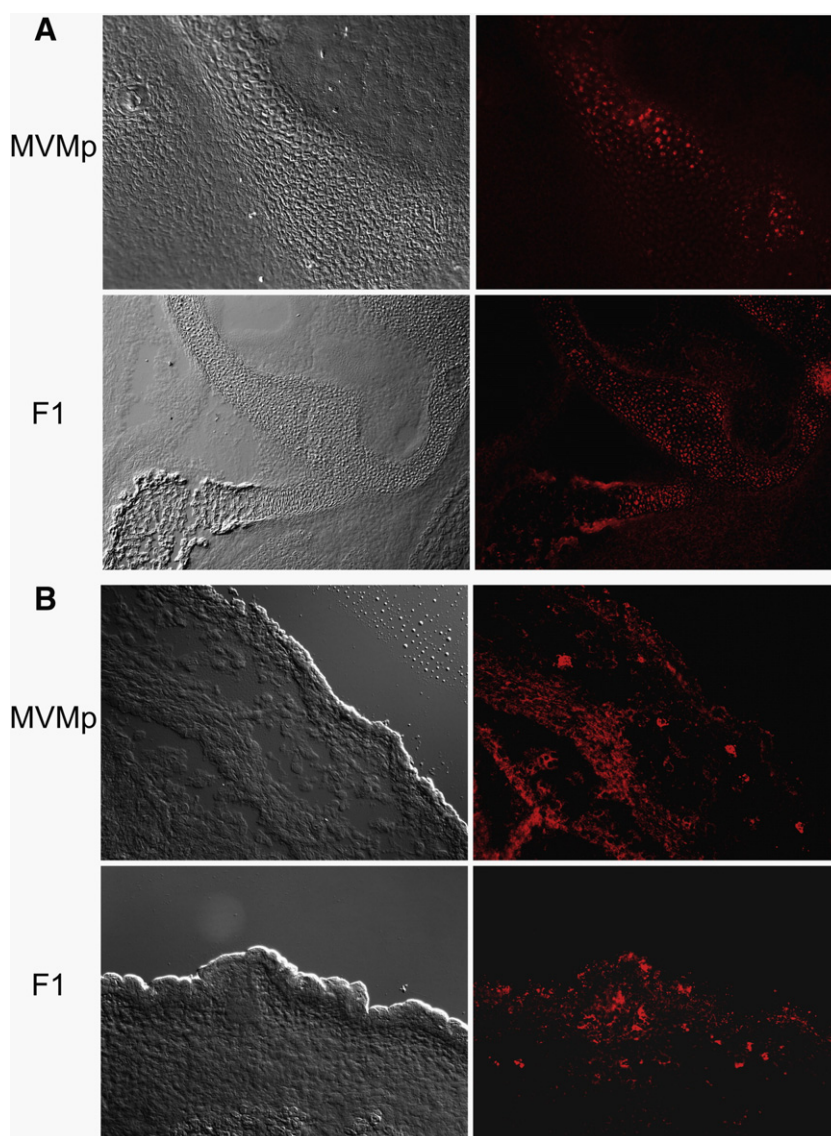
Fig. 7. Histological distribution of MVMp and F1 infections in mice embryonic tissues. Embryos were injected through uterine wall and further processed as described in Materials and methods. The sample data is represented in pairs of DIC images (left panels) and Fluorescence images, showing distribution of viral capsids (right panels). Typical transverse sections through primordial bone (A) and skin (B) tissues are represented.

the same region of the capsid responsible for determining the reciprocal tropism of the fibrotropic (MVMp) and lymphotropic (MVMi) strains of MVM, and adjacent to residues identified in virulent MVMp mutants isolated from SCID mice (López-Bueno et al., 2006a). Two of four VP F1-specific mutations (334 and 384 VP2 amino acid positions) are located within the MVM fibrotropic determinant region (Gardiner and Tattersall, 1988), with the E384 side-chain performing a stabilizing role for a surface loop through its interactions with the main-chain of MVMi/p differing residue S388 contained within this loop. Mutations of residues in a homologous loop to this one in canine parvovirus at amino acid positions K387A and T389 to alanine in CPV have been reported to result in a non-infectious CPV phenotype (Parker and Parrish, 1997). The remaining two residues, N554 and I578 are structurally clustered adjacent to other MVMi/p differing residues, VP2 residue mutations (399, 460, 553, 558) known to be involved in adaptation of MVMi to A9 fibroblasts and MVMp amino acids (362, 368, 551, 575) that mutate in SCID mice to confer a virulent phenotype to this otherwise non-pathogenic virus (Agbandje-McKenna et al., 1998, Kontou et al., 2005, López-Bueno et al., 2006a). These ob-

servations suggest that local capsid surface topology changes, resulting from these mutations of the MVMp residues to those observed in F1, facilitate host range adaptation. The location of all the F1 capsid mutations at or close to the capsid surface pocket where MVM is predicted to binds its sialic acid receptor further supports the possibility of extension of MVM host range by adaptation of its structural tissue tropism and pathogenicity determinants to a new host.

Despite the location of the F1 residues close to the MVM receptor binding site, binding affinity does not appear to be altered in the mutant virus as determined by the similar levels of genomic DNA isolated from infected cells 1 h post infection (Fig. 5). This observation supports a restrictive block post entry that involves a capsid-mediate interaction/dynamic that is not yet identified as is the difference between WT MVMp and MVMi. This phenotype differs from that observed for MVMp adaptation to a virulence phenotype, which resulted in decreased affinity for the cell surface sialic acid, and an increased viral spread consistent with a large plaque phenotype compared to the WT MVMp (López-Bueno et al., 2006a; Nam et al., 2006). Significantly, the localization of the VP2

residues implicated in the F1 adaptation at the icosahedral two-fold axis is consistent with other tissue tropism and pathogenicity determinants for parvoviruses in general (reviewed in Kontou et al., 2005), and further implicates the parvoviral two-fold region in this phenomenon.

The silent G1955A substitution is found in the region known to regulate large-intron splicing (Pintel et al., 1995). Substitutions within this region have been shown to affect large-intron splicing in a cell-dependent manner. MVMi carrying one of the silent G1967A or G1970A was demonstrated to increase NS2 levels in A9 fibroblasts (D'Abramo et al., 2005). The interaction between adenosine at the splicing branch point and the U2 snRNA is crucial for splicing (Moore et al., 1993). The G1970A substitution in MVMi was demonstrated to significantly improve large-intron splicing and increase both R2 and NS2 levels in A9 fibroblasts by modifying the interaction with endogenous U2 snRNA (Choi et al., 2005). It is therefore similarly possible that the substituted adenosine at nt 1955 alters binding of U2 snRNA to the large-intron splicing branch point in F111 rat fibroblasts. The significantly enhanced production of R2 and NS2 by F1 in F111 supports this hypothesis. NS2 is known to be involved in several MVM functions such as virus DNA replication (Naeger et al., 1990), mRNA translation (Naeger et al., 1993), nuclear egress of progeny virions in mouse cells (Eichwald et al., 2002) and particle assembly (Cotmore et al., 1997).

Current study does not reveal what mutation/s or their combination can be sufficient for the virus–host range switch from mouse to rat fibroblasts. Lymphotropic MVMi was demonstrated to require at least two capsid amino acid alternations associated with sialic acid binding region in order to adapt to A9 fibroblasts (Ball-Goodrich and Tattersall, 1992; Agbandje-McKenna et al., 1998). Alternatively fibrotropism can be conferred to MVMi by combination of one of the silent substitutions facilitating NS2 production (G1967A or G1970A) and one of the additional VP2 amino acid changes at the position 399 (D399G or D399A) (D'Abramo et al., 2005). Thus we think that the extension of our study possibly can reveal very limited number of genomic changes in MVM genome, conferring *trans*-species host range change to the virus.

Specificity of the F1 host range

Several lines of evidence indicate considerable differences between host-range properties of the WT MVMp and the F1 mutant. In vitro, F1 infection at even a low multiplicity (0.2 PFU/cell) efficiently destroyed F111 rat fibroblasts culture, whereas infection of these cells with a high multiplicity of WT MVMp (2 PFU/cell) caused only a slight CPE, followed by full recovery of the culture. DNA replication and genome expression of F1 were significantly better in F111 cells, while the WT MVMp had a substantial advantage in A9 and NB324K. Although the mutant viruses were selected in a rat tissue culture host, we showed that F1 was able to infect mouse embryos *in utero* and that there was significant divergence between the WT MVMp and F1 mutants in their infection properties. Finally F1-specific mutations were preserved only during propagation in F111 cells; passaging in A9 and NB324K cultures resulted in reversion to the WT MVMp pattern. Interestingly, even PyF cells, which are transformed F111 cells and therefore of rat origin, were more supportive of WT MVMp than F1 infection, indicating the high specificity of the cellular factors determining parvovirus tropism and highlighting the effect of transformation on the biology of the autonomous parvoviruses.

We suggest that further studies in this direction could lead to generation of autonomous parvoviruses with desired host range properties, permitting construction of gene therapy vectors with determined targeting and a better understanding of the role of cell transformation in determining the characteristics of parvovirus-host cell biology.

Materials and methods

Cell culture

A9 mouse fibroblast cells (Littlefield, 1964), NB324K simian virus 40-transformed human newborn kidney cells (Shein and Enders, 1962), F111 Fisher rat fibroblasts (Freeman et al., 1973), and PyF polyomavirus-transformed F111 cells (Guetta et al., 1990) were cultured in monolayers in Dulbecco modified Eagle medium (Gibco Laboratories) supplemented with 5% inactivated fetal bovine serum at 37 °C, 5% CO_2.

Virus

MVMp was produced by transfection (see below) of its infectious clone pMM984 (Merchlinsky et al., 1983) into A9 cells. After cell death, virus was extracted by standard procedure (Tattersall et al., 1976) and was not further passaged.

F1 mutant virus was produced by end point dilution of the MVMp-F111 isolate (see "Results") in F111 cells followed by subsequent propagation in these cells. Typically 10^6 cells in a 150 mm plate were infected with 10^{-2} PFU/cell and ~10^7 PFU/plate was obtained. Resulting virus was checked by direct PCR and sequencing as well as by sequencing of its Plaque Purified isolates. In addition, F1 stocks were routinely checked by ARMS (see below). All controls did not reveal genomic heterogeneity.

Transfections and Infections

All transfections/co-transfections were done with FuGENE 6 transfection reagent according to the manufacturer's (Roche) protocol. For MVMp infections, the desired host cells were seeded and 12 h later the growth medium was replaced by Dulbecco modified Eagle medium without serum (1/10 of a normal volume), containing active viral particles at the desired multiplicity of infection (MOI). After 1 h incubation with gentle shaking under the standard cell growth conditions (see above), the inoculum was removed, cells were washed with PBS and grown under the standard conditions (see above). For virus passage experiments, 10^6 cells were infected with 0.2 PFU/cell and cultured until cell death. Virus extracted was subsequently used for a further infection of the same cell-type with the same MOI.

Plaque assays/purification

Standard procedure (Tattersall and Bratton, 1983) was used to determine the amount of active virus particles (PFU) in our viral samples. Plaque purification was performed as described elsewhere (Tattersall, 1972). End point dilutions of mutant viruses in F111 cells were performed in 96 well plates according to general protocol (Mahy and Kangro, 1996).

PCR assays

Viral templates for PCR were treated with 20 μg/ml DNAse (NEB) for 1 h to remove contaminating genomic and viral Replicative Form DNAs.

To amplify the coding sequences of the MVM genome by a single reaction, the F117 (ATAAGCGGTTCAGGGAGTTTA) and R4928 (CTGAATAGACAGTAGTCTTGGTTGAG) primers were used in the Expand Long Template PCR System (Roche). A prolonged initial denaturation of 95 °C for 10 min was introduced to destroy viral capsids. 35 thermal cycles consisting of denaturation at 95 °C for 45 s, annealing at 55 °C for 30 s, elongation at 72 °C for 5 min followed by a final elongation at 72 °C for 15 min were performed.

Amplification-Refractory Mutation System (ARMS) allele-specific PCR (Newton et al., 1989) included one constant unselective primer

Table 3
Primer sets used for ARMS

Genome position (bp)	SNP	Allele-specific primers (name and sequence)	Unselective primer (name and sequence)	Reaction annealing temp. (°C)	Product size (bp)
1955	G — WT	R1974-WT; 5′gagttggcacctttggctac	F1629; 5′gccatttgctctggtcaaactat	61	345
	A — mutant	R1974-M; 5′gagttggcacctttggctat			
3793	G — WT	R3814-WT; 5′gttgacaaaatcctacttgatc	F3449; 5′gagatctttcagtgacctacg	54	365
	A — mutant	R3814-M; 5′gttgacaaaatcctacttgatt			
3944	A — WT	R3961-WT; 5′catgtgaagcccaattat	F3449; 5′gagatctttcagtgacctacg	53	512
	C — mutant	R3961-M; 5′catgtgaagcccaattag			
4453	A — WT	R4473-WT; 5′actcatgtatgagttgccagt	F4092; 5′ccctattgggactaaaaatgac	58	381
	G — mutant	R4473-M; 5′actcatgtatgagttgccagc			
4525	A — WT	R4544-WT; 5′ctagcaacaggtcttgttgt	F4092; 5′ccctattgggactaaaaatgac	56	452
	C — mutant	R4544-M; 5′ctagcaacaggtcttgttgg			

Single nucleotide polymorphisms (SNP) at the indicated mutant loci were checked for each one of the depicted genome positions by two allele-specific PCRs. Each reaction employed one of the shown selective allele-specific primers, (one designed to specifically amplify the wild-type [WT] and another the mutant [M] templates), along with the corresponding unselective primer.

and one allele-specific primer (Table 3). An initial denaturation of 95 °C for 10 min was used to destroy the viral capsids. Amplification consisted of 35 cycles of denaturation at 95 °C for 30 s, annealing for 30 s at a temperatures specific for each reaction (Table 3), and elongation at 72 °C for 30 s. A final elongation at 72 °C for 2 min was included. All reactions were performed in 50 µl volumes. Each reaction contained: 1 U of Taq polymerase (Super-Nova), 5 µl of 10X Taq buffer supplemented with 15 mM MgCl$_2$ (Super-Nova), 100 µM each of dNTPs, 0.1 µM each of a selective and an unselective primer. Reaction products and a 100 bp DNA Ladder (NEB) were resolved by agarose gel (1.5%) electrophoresis (5 V/cm) and identified by staining with EtBr.

Four test templates for the ARMS allele-specific PCR assay were constructed. pVP-WT and pVP-F1 were made by PCR amplification of the region 3449-4867 in WT MVMp and F1 DNA respectively, using the primers F3449 (see Table 3) and R4867-EcoRI (CATCAAGTCTAAGGGAATTCC), which introduced an EcoRI endonuclease restriction site into the PCR product. The EcoRI-cut product was then cloned into the EcoRI site of the plasmid pGEM (Promega). To produce pP38-WT/pP38-1955, MVMp/F1 PCR-amplified DNA sequences, between two EcoRI sites (located at positions 1084 and 3522 of the MVM genome) were cloned into the EcoRI site of pGEM.

Sequencing

PCR products were purified by the QIAGEN PCR Purification Kit and sequenced by standard chain-terminator methods. Sets of primers, located less than 500 bp from each other and covering the whole 117–4928 bp PCR product (see above) was employed to permit the sequencing of the entire amplified region. To avoid mistakes, at least two PCR products from separate reactions were sequenced for all viral samples. The sequence of MVMp infectious clone pMM984 (Merchlinsky et al., 1983) was determined between 117 and 4928 bp of the MVMp genome. This sequence was aligned with DNA sequencing results of the samples of interest, using the NCBI BLAST online software. NCBI BLASTX was used to determine amino acid changes caused by identified DNA mutations.

Structural analysis of mutated residues

The coordinates for the MVMp VP2 crystal structure (Kontou et al., 2005) (PDB accession number 1z14) was used to map the positions of the mutated residues onto the MVMp capsid. The icosahedral two-, three- and five-fold related monomers were generated by applying icosahedral symmetry operators to a reference monomer using the program O (Jones et al., 1991) on a Silicon graphics Octane workstation. The positions of the mutated residues were visualized and analyzed in the context of the viral capsid using the program COOT

(Emsley and Cowtan, 2004), and graphically presented using the program PyMOL (DeLano, 2002).

CAT transfection assays

CAT reporter sequence under the control of WT and mutant P38 promoters were constructed as follows. pP38[WT]-CAT was constructed by sub-cloning the Eco RV/Hpa II restriction endonuclease fragment (nt 383–5042 of MVMp) taken from pMM984 (Merchlinsky et al., 1983), into the pGEM plasmid (Promega) EcoRV site. Within this subclone the sequence between nt 2650 and 4212 was released by cleavage with Hind III and BglII, and the CAT coding sequence, released from pTS1 (Tratschin et al., 1986) with the same enzymes, was substituted in its place. Mutant pP38[1955]-CAT was made by substituting the WT MVM sequence between BstEII (1884 bp) and XhoI (2070 bp) in pP38[WT]-CAT with sequence derived from PCR-amplified F1 virus DNA. pNS was constructed by releasing the NS coding region from pMM984 (Merchlinsky et al., 1983) by cleavage with BamHI and Hind and cloning into the pGEM EcoRV site.

All transfection experiments were performed in triplicate. 10⁵ cells, seeded 12 h previously, in 6 well plates were co-transfected with one of the CAT reporter constructs (pP38[WT]-CAT or pP38 [1955]-CAT) (500 ng/well), pNS (250 ng/well), and pSV2βgal (Promega) (250 ng/well) as an internal control. 48 hpt cells were harvested and 100 µl extract volumes were assayed for CAT and β-gal activities (Gorman et al., 1982; Settleman and DiMaio, 1988). The level of chloramphenicol acetylation was determined by overnight exposure of thin-layer chromatography plates to a phosphor-imager screen (FUJIFILM FLA-5100). Signal strengths of acetylated and non-acetylated chloramphenicol forms were quantified with Image Gauge software. The transfection efficiency was calculated from the specific activity of β-galactosidase present in each extract.

Cell survival assay

MTT assays were performed in 96 well plates according to the original protocol (Pauwels et al., 1988). OD values were adjusted to the confluence of living cells of all types.

Southern analysis

1 or 20 hpi cells were washed with PBS and low molecular DNA was extracted by the Hirt method (McMaster et al., 1981). Viral DNA and Lambda DNA-HindIII marker (NEB) were resolved by agarose gel (0.8%) electrophoresis (5 V/cm), capillary transferred (Sambrook and Russel, 2001) to a NytranN nylon membrane (Schleicher & Schuell BioScience) and hybridized according to the manufacturer's protocol to a mixed probe of MVMp full-length genome and Lambda DNA, labeled by

random priming with ^{32}P. After hybridization, membranes were exposed to phosphor-imager screens (5 h) with subsequent development by the phosphor-imager (FUJIFILM FLA-5100).

Northern analysis

mRNA of infected cells was extracted by the mRNA Direct Kit (Chemagen) 14 hpi and quantified spectrophotometrically. Equal amounts of mRNA from each sample were resolved with prolonged (8 h) electrophoresis (2 V/cm) in 1% agarose gels, containing 2.2 M formaldehyde following a standard protocol (Sambrook and Russel, 2001). RNA was then capillarily transferred to NytranN nylon membranes (Schleicher & Schuell BioScience) and hybridized according to the manufacturer's protocol to an MVMp genomic DNA probe labeled by random priming with ^{32}P. Images were developed by the phosphor-imager as described for the Southern.

Western analysis

24 hpi total protein extraction was performed with RIPA buffer (Bio-Rad) and quantified by a modified Bradford assay (Bio-Rad Protein Assay Dye). Equal amounts of proteins from different samples were resolved by discontinuous SDS-Polyacrylamide gel (8% for VP, 10% for NS proteins) electrophoresis and electrophoretically transferred to nitrocellulose membranes (Amersham Biotech), using a Bio-Rad Mini-PROTEAN device, according to the manufacturer's protocols. Immunoassaying was performed according to the standard protocol (Sambrook and Russel, 2001), using rabbit-raised polyclonal primary antibodies for VP and NS proteins, kindly provided by Jean Rommelaere (German Cancer Research Center) and Peroxidase-labeled anti-rabbit secondary Ab (Amersham Biotech). ECL was performed with Western Blotting Luminol Reagent (Santa Cruz) and membranes were exposed to Kodak ML films for 1 min.

In vivo infections

Neonate mice less than 16 h old were inoculated oral-nasally with 10^3 PFU/mouse of virus in 4 μl of saline. 12 dpc mouse embryos were inoculated by injection of 10^5 PFU/embryo of virus into the embryonic liver *in utero* as described previously (Itah et al., 2004a). After a further 48 hour incubation, both newborns and embryos were dissected, embedded in Optimal Cutting Temperature (OCT), cryosectioned, and the sections were mounted on slides. MVM capsid protein distribution in the tissues was determined by immunohistochemistry using polyclonal anti-MVM capsid antisera as described previously (Itah et al., 2004b).

Acknowledgments

Appendix A. Supplementary data

Supplementary data associated with this article can be found, in the online version, at doi:10.1016/j.virol.2008.06.042.

References

Ball-Goodrich, L.J., Tattersall, P., 1992. Two amino acid substitutions within the capsid are coordinately required for acquisition of fibrotropism by the lymphotropic strain of minute virus of mice. J. Virol. 66 (6), 3415–3423.

Choi, E.Y., Newman, A.E., Burger, L., Pintel, D., 2005. Replication of minute virus of mice DNA is critically dependent on accumulated levels of NS2. J. Virol. 79 (19), 12375–12381.

Cornelis, J.J., Dinsart, C., 2006. Helper-independent parvoviruses as gene therapy and vaccine delivery vectors. In: Kerr, J.R., Cotmore, S.F., Bloom, M.E., Linden, R.M., Parrish, C.R. (Eds.), Parvoviruses. Hodder Arnold, London, pp. 571–583.

Cornelis, J.J., Deleu, L., Koch, U., Rommelaere, J., 2006. Parvovirus oncosuppression. In: Kerr, J.R., Cotmore, S.F., Bloom, M.E., Linden, R.M., Parrish, C.R. (Eds.), Parvoviruses. Hodder Arnold, London, pp. 365–378.

Cotmore, S.F., Tattersall, P., 1986. Organization of nonstructural genes of the autonomous parvovirus minute virus of mice. J. Virol. 58 (3), 724–732.

Cotmore, S.F., Tattersall, P., 2006. A rolling-hairpin strategy: basic mechanisms of DNA replication in the parvoviruses. In: Kerr, J.R., Cotmore, S.F., Bloom, M.E., Linden, R.M., Parrish, C.R. (Eds.), Parvoviruses. Hodder Arnold, London, pp. 171–188.

Cotmore, S.F., Christensen, J., Nüesch, J.P., Tattersall, P., 1995. The NS1 polypeptide of the murine parvovirus minute virus of mice binds to DNA sequences containing the motif [ACCA]2-3. J. Virol. 69 (3), 1652–1660.

Cotmore, S.F., D'Abramo Jr., A.M., Carbonell, L.F., Bratton, J., Tattersall, P., 1997. The NS2 polypeptide of parvovirus MVM is required for capsid assembly in murine cells. Virology 231 (2), 267–280.

D'Abramo Jr., A.M., Ali, A.A., Wang, F., Cotmore, S.F., Tattersall, P., 2005. Host range mutants of Minute Virus of Mice with a single VP2 amino acid change require additional silent mutations that regulate NS2 accumulation. Virology 340 (1), 143–154.

DeLano, W.L., 2002. The PyMOL Molecular Graphics System. DeLano Scientific, San Carlos, CA, USA.

Doerig, C., Hirt, B., Beard, P., Antonietti, J.P., 1988. Minute Virus of Mice non-structural protein NS1 is necessary and sufficient for *trans*-activation of the viral P39 promoter. J. Gen. Virol. 69, 2563–2573.

Eichwald, V., Daeffler, L., Klein, M., Rommelaere, J., Salomé, N., 2002. The NS2 proteins of parvovirus minute virus of mice are required for efficient nuclear egress of progeny virions in mouse cells. J. Virol. 76 (20), 10307–10319.

Emsley, P., Cowtan, K., 2004. Coot: model-building tools for molecular graphics. Acta Crystallogr D Biol Crystallogr 60, 2126–2132.

Faisst, S., Perros, M., Deleu, L., Spruyt, N., Rommelaere, J., 1994. Mapping of upstream regulatory elements in the P4 promoter of parvovirus minute virus of mice. Virology 202 (1), 466–470.

Freeman, A.E., Gilden, R.V., Vernon, M.L., Wolford, R.G., Hugunin, P.E., Huebner, R.J., 1973. 5-Bromo-2′-deoxyuridine potentiation of transformation of rat-embryo cells induced in vitro by 3-methylcholanthrene: induction of rat leukemia virus gs antigen in transformed cells. Proc. Natl. Acad. Sci. U. S. A. 70 (8), 2415–2419.

Gardiner, E.M., Tattersall, P., 1988. Mapping of the fibrotropic and lymphotropic host range determinants of the parvovirus minute virus of mice. J. Virol. 62 (8), 2605–2613.

Gorman, C.M., Moffat, L.F., Howard, B.H., 1982. Recombinant genomes which express chloramphenicol acetyltransferase in mammalian cells. Mol. Cell Biol. 2 (9), 1044–1051.

Guetta, E., Mincberg, M., Mousset, S., Bertinchamps, C., Rommelaere, J., Tal, J., 1990. Selective killing of transformed rat cells by minute virus of mice does not require infectious virus production. J. Virol. 64 (1), 458–462.

Itah, R., Gitelman, I., Tal, J., Davis, C., 2004a. Viral inoculation of mouse embryos in utero. J. Virol. Methods 120 (1), 1–8.

Itah, R., Tal, J., Davis, C., 2004b. Host cell specificity of minute virus of mice in the developing mouse embryo. J. Virol. 78 (17), 9474–9486.

Jones, T.A., Zou, J.Y., Cowan, S.W., Kjeldgaard, M., 1991. Improved methods for building protein models in electron density maps and the location of errors in these models. Acta Crystallogr. A. 47, 110–119.

Kimsey, P.B., Engers, H.D., Hirt, B., Jongeneel, C.V., 1986. Pathogenicity of fibroblast- and lymphocyte-specific variants of minute virus of mice. J. Virol. 59 (1), 8–13.

Kontou, M., Govindasamy, L., Nam, H.J., Bryant, N., Llamas-Saiz, A.L., Foces-Foces, C., Hernando, E., Rubio, M.P., McKenna, R., Almendral, J.M., Agbandje-McKenna, M., 2005. Structural determinants of tissue tropism and in vivo pathogenicity for the parvovirus minute virus of mice. J. Virol. 79 (17), 10931–10943.

Littlefield, J.W., 1964. Three degrees of guanylic acidinosinic acid pyrophosphorylase deficiency in mouse fibroblasts. Nature 203, 1142–1144.

López-Bueno, A., Mateu, M.G., Almendral, J.M., 2003. High mutant frequency in populations of a DNA virus allows evasion from antibody therapy in an immunodeficient host. J. Virol. 77 (4), 2701–2708.

López-Bueno, A., Rubio, M.P., Bryant, N., McKenna, R., Agbandje-McKenna, M., Almendral, J.M., 2006a. Host-selected amino acid changes at the sialic acid binding pocket of the parvovirus capsid modulate cell binding affinity and determine virulence. J. Virol. 80 (3), 1563–1573.

López-Bueno, A., Villarreal, L.P., Almendral, J.M., 2006b. Parvovirus variation for disease: a difference with RNA viruses? Curr. Top Microbiol. Immunol. 299, 349–370.

Lorson, C., Pintel, D.J., 1997. Characterization of the minute virus of mice P38 core promoter elements. J. Virol. 71 (9), 6568–6575.

Mahy, B.W.J., Kangro, H.O., 1996. Virology Methods Manual, First edition. Academic Press, New York.

McMaster, G.K., Beard, P., Engers, H.D., Hirt, B., 1981. Characterization of an immunosuppressive parvovirus related to the minute virus of mice. J. Virol. 38 (1), 317–326.

Merchlinsky, M.J., Tattersall, P.J., Leary, J.J., Cotmore, S.F., Gardiner, E.M., Ward, D.C., 1983. Construction of an infectious molecular clone of the autonomous parvovirus minute virus of mice. J. Virol. 47 (1), 227–232.

Agbandje-McKenna, M., Llamas-Saiz, A.L., Wang, F., Tattersall, P., Rossmann, M.G., 1998. Functional implications of the structure of the murine parvovirus, minute virus of mice. Structure 6 (11), 1369–1381.

Moore, M.J., Query, C.C., Sharp, P.A., 1993. Splicing of precursors to mRNA by the spliceosome. In: Gesteland, R., Atkins, J. (Eds.), The RNA World. Cold Spring Harbor Laboratory Press, Cold Spring Harbor, NY.

Naeger, L.K., Cater, J., Pintel, D.J., 1990. The small nonstructural protein (NS2) of the parvovirus minute virus of mice is required for efficient DNA replication and infectious virus production in a cell-type-specific manner. J. Virol. 64, 6166–6175.

Naeger, L.K., Salomé, N., Pintel, D.J., 1993. NS2 is required for efficient translation of viral mRNA in minute virus of mice-infected murine cells. J. Virol. 67 (2), 1034–1043.

Nam, H.J., Gurda-Whitaker, B., Gan, W.Y., Ilaria, S., McKenna, R., Mehta, P., Alvarez, R.A., Agbandje-McKenna, M., 2006. Identification of the sialic acid structures recognized by minute virus of mice and the role of binding affinity in virulence adaptation. J. Biol. Chem. 281 (35), 25670–25677.

Newton, C.R., Graham, A., Heptinstall, L.E., Powell, S.J., Summers, C., Kalsheker, N., Smith, J.C., Markham, A.F., 1989. Analysis of any point mutation in DNA. The amplification refractory mutation system (ARMS). Nucleic Acids Res. 17 (7), 2503–2516.

Nuesch, J.P.F., 2006. Regulation of non-structural protein functions by differential synthesis, modification and trafficking. In: Kerr, J.R., Cotmore, S.F., Bloom, M.E., Linden, R.M., Parrish, C.R. (Eds.), Parvoviruses. Hodder Arnold, London, pp. 275–289.

Parker, J.S., Parrish, C.R., 1997. Canine parvovirus host range is determined by the specific conformation of an additional region of the capsid. J. Virol. 71 (12), 9214–9222.

Parrish, C.R., Hueffer, K., 2006. Parvovirus host range, cell tropism and evolution — studies of canine and feline parvoviruses, minute virus of mice, porcine parvovirus, and Aleutian mink disease virus. In: Kerr, J.R., Cotmore, S.F., Bloom, M.E., Linden, R.M., Parrish, C.R. (Eds.), Parvoviruses. Hodder Arnold, London, pp. 343–351.

Pauwels, R., Balzarini, J., Baba, M., Snoeck, R., Schols, D., Herdewijn, P., Desmyter, J., De Clercq, E., 1988. Rapid and automated tetrazolium-based colorimetric assay for the detection of anti-HIV compounds. J. Virol. Methods 20 (4), 309–321.

Pintel, D., Dadachanji, D., Astell, C.R., Ward, D.C., 1983. The genome of minute virus of mice, an autonomous parvovirus, encodes two overlapping transcription units. Nucleic Acids Res. 11 (4), 1019–1038.

Pintel, D., Gersappe, A., Haut, D., Pearson, J., 1995. Determinants that govern alternative splicing of parvovirus pre-mRNAs. Semin. Virol. 6, 283–290.

Previsani, N., Fontana, S., Hirt, B., Beard, P., 1997. Growth of the parvovirus minute virus of mice MVMp3 in EL4 lymphocytes is restricted after cell entry and before viral DNA amplification: cell-specific differences in virus uncoating in vitro. J. Virol. 71, 7769–7780.

Qiu, J., Yoto, Y., Tullis, G., Pintel, D., 2006. Parvovirus RNA processing strategies. In: Kerr, J.R., Cotmore, S.F., Bloom, M.E., Linden, R.M., Parrish, C.R. (Eds.), Parvoviruses. Hodder Arnold, London, pp. 253–275.

Ron, D., Tattersall, P., Tal, J., 1984. Formation of a host range mutant of the lymphotropic strain of minute virus of mice during persistent infection in mouse L-cells. J. Virol. 52, 63–69.

Sambrook, J., Russel, D.W., 2001. Molecular Cloning: a Laboratory Manual. Cold Spring Harbor, New York.

Shein, H., Enders, J.F., 1962. Multiplication and cytopathogenicity of Simian vacuolating virus 40 in cultures of human tissues. Proc. Soc. Exp. Biol. Med. 109, 495–500.

Settleman, J., DiMaio, D., 1988. Efficient transactivation and morphologic transformation by bovine papilloma genes expressed from bovine papillomavirus/simian virus 40 recombinant virus. Proc. Natl. Acad. Sci. USA 85, 9007–9011.

Spalholz, B.A., Tattersall, P., 1983. Interaction of minute virus of mice with differentiated cells: strain-dependent target cell specificity is mediated by intracellular factors. J. Virol. 46, 937–943.

Tattersall, P., 1972. Replication of the parvovirus MVM. J. Virol. 10, 586–590.

Tattersall, P., 2006. The evolution of parvovirus taxonomy. In: Kerr, J.R., Cotmore, S.F., Bloom, M.E., Linden, R.M., Parrish, C.R. (Eds.), Parvoviruses. Hodder Arnold, London, pp. 5–14.

Tattersall, P., Bratton, J., 1983. Reciprocal productive and restrictive virus–cell interaction of immunosuppressive and prototype strains of minute virus of mice. J. Virol. 46, 944–955.

Tattersall, P., Cawte, P.J., Shatkin, A.J., Ward, D., 1976. Three structural polypeptides coded for by Minute Virus of Mice, a parvovirus. J. Virol. 20, 273–289.

Tattersall, P., Shatkin, A.J., Ward, D., 1977. Sequence homology between the structural polypeptides of minute virus of mice. J. Mol. Biol. 111 (4), 375–394.

Tratschin, J.D., Tal, J., Carter, B.J., 1986. Negative and positive regulation in trans of gene expression from adeno-associated virus vectors in mammalian cells by a viral rep gene product. Mol. Cell Biol. 6 (8), 2884–2894.